


Research Article

Uncertainty Analysis of Energy Production for a 3×50 MW AC Photovoltaic Project Based on Solar Resources

Irfan Jamil ¹, Jinquan Zhao,¹ Li Zhang,¹ Syed Furqan Rafique,² and Rehan Jamil³

¹College of Energy and Electrical Engineering, Hohai University, Nanjing, China

²PV Overseas Management Center, GCL New Energy, Suzhou, China

³Solar/Wind International Business Department, TBEA Xinjiang Sunoasis Co. Ltd., Urumqi, China

Correspondence should be addressed to Irfan Jamil; i.jamil@hhu.edu.cn

Received 3 September 2018; Revised 9 November 2018; Accepted 14 November 2018; Published 4 February 2019

Academic Editor: Huiqing Wen

Copyright © 2019 Irfan Jamil et al. This is an open access article distributed under the Creative Commons Attribution License, which permits unrestricted use, distribution, and reproduction in any medium, provided the original work is properly cited.

Access to solar energy is a prerequisite to remedy CO₂ and improve the standard of human living. Green solar energy is only an immediate solution to add its zero emission profile and provide carbon footprint reduction benefits. This energy does not emit greenhouse gases which means it is a renewable free source of energy when producing electricity. The purpose of this paper is to investigate the accurate annual energy production data reducing uncertainty in solar energy estimates. This work investigated the solar energy assessment taking into account a detailed solar resource and energy production assessment for a 3×50 MW PV project with uncertainty analysis. The authors defined a total uncertainty of energy production which is estimated at 9.5% for one year and 8.9% for ten years as well as future variability of 3.4% for one year and 1.1% for ten years. The annual power degradation and expected energy production over the plant lifespan at dissimilar 99%, 90%, 75%, 60%, 50%, and 25% probability of surplus are also observed in this paper.

1. Introduction

Pakistan is confronting issues of acute shortage of electricity and energy supply demand. About 43% of the total population of Pakistan lives without access to electricity, and approximately 50,000 villages are completely detached from the national grid [1]. The GoP has tasked the province's energy department for the provision of a requisite institutional framework to end the shortage of energy supply. The energy department's domain, inter alia, includes the generation of electricity by exploring especially indigenous resources, including solar, wind, biomass, and hydro. A master plan was developed by the GoP to issue many LOIs to solar energy developers for the development of large-scale solar power plants because PV technology is a promising application of renewable energy, widely used in urban and remote areas [2]. Within the master plan, first step is an overview of solar information, investigating the resources, rights and general information. According to the PV installation environment, PV power-generating systems are divided into on-grid-connected and off-grid-connected PV systems. The

original concept of the master plan is acquired to install an on-grid-connected project and grid-connected solar PV system which is the fastest-growing power-generating technology today [3, 4]. In this case, an installed capacity of 3×50 MW is selected, which would be able to produce electricity energy for about 150,000 homes during peak daytime hours [5]. Through this project, the authors intend to create awareness amongst the general public for the use of renewable energy resources to reduce the burden on the national grid and to improve environmental conditions of the province. In the development of PV projects, the major area of risk is quantifying the expected annual energy production and uncertainty analysis whereas the most significant driver is the uncertainty in solar irradiance. Solar project developers require reasonable information in energy yield predictions in order to reduce the cost of financing systems, to understand the PV modeling uncertainty [6]. The flow of energy yield in the PV modeling chain is also discussed further. For this purpose, a feasibility study of a project was performed with the aim of performing the following tasks:

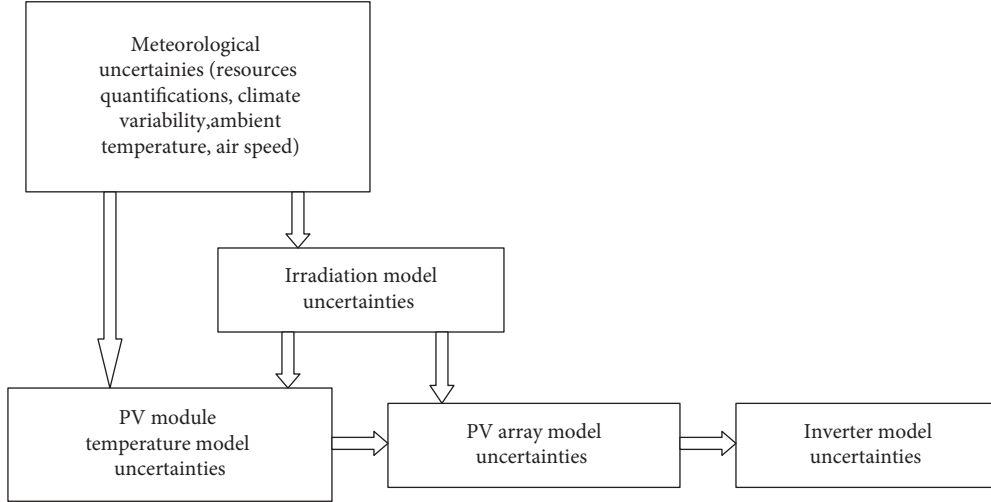


FIGURE 1: Different steps in the PV modeling chain.

- (i) Review different solar resources and evaluation of energy production of 3×50 MW with respect to uncertainty analysis
- (ii) Provision of the requirements of the photovoltaic systems to meet the identified design profiles and equipment selection

The following uncertainly/elements and assemblies are subject to investigation as preparatory work.

1.1. Uncertainty in the PV Modeling Chain. Different performance models are applied in the industry to anticipate the measure of energy amount that the PV system can produce. These diverse models can differ significantly in their underlying mathematical formulations, in the numerical approach, and in the amount of data (assumptions) required for the simulation. The different steps in the PV modeling chain are subject to uncertainties as shown in Figure 1. The uncertainties affect different steps of the whole PV system parameters such as on meteorological, irradiation, PV module temperature, PV array, and inverter. The uncertainties on the environmental conditions are moderately larger while assessing the PV energy yield [7].

1.2. Technical/Financial Risk Factors. The technical risk factors in solar power generation depend on the perspective of the different stakeholders and their physical liability in the socioeconomic sector. When they start the development of renewable energy technology, they go over technical and financial risk assessments in terms of the technology they applied. Herein, we take into consideration technical risk factors for 3×50 MW which are an important uncertainty for identification from the perspective of solar developers [8]. The uncertainty of solar resource has great impact on financial risk factors. To manage the financial risk assessment of an investment in a grid-connected PV system, the uncertainty quantification of solar energy yield calculation is identified, which is an important case based on the energy flow in the PV modeling chain. These uncertainties in solar

resources are subjected to climate variability (σ_{Clim}), irradiation quantification (σ_{Irr}), conversion to the plane-of-array ($\sigma_{\text{POA-conv}}$), temperature modeling (σ_{Temp}), PV array modeling (σ_{PVarr}), inverter modeling (σ_{Inv}), PV field-related uncertainties (σ_{Fld}), DC cabling ($\sigma_{\text{C-DC}}$), AC cabling ($\sigma_{\text{C-AC}}$), and availability (σ_{Av}) highlighted in the different steps of the main energy conversion in a PV system. Thus, given the parameters in Figure 2, if we maintain with correct quantification all uncertainties in the PV system modeling, then the financial risk assessment will allow the developers and investors to contain this factor [7].

1.3. PV Yield Assessment. We used the PVsyst package along with internal tools to calculate an energy yield assessment and expected production, which gives the right input data for the PV system [9].

1.4. Project Profile. Pakistan lies at a high potential solar radiation belt, and the land is available in large-scale magnitude for the development of solar power projects. The 3×50 MW site has an evacuation facility of 220 kV grid and is located 115 km northeast of Karachi, Pakistan, near the town of Thano Bula Khan and Nooriabad, Sindh. The 3×50 MW site is composed of three (3) identical projects which are located in combination in the same parcel of land side by side. Based on land coordinates, the site has a rich sun-radiation impact [5]. The physical condition of the project land can be viewed in Figure 3.

The site coordinates with latitude and longitude are given below in Table 1.

1.5. Solar Resource Assessment. The solar energy resource assessment is the key role in the development of large scale-sized solar projects [10, 11]. The best way to determine the solar irradiation and temperature data at a particular site is by measuring different parameters of interest with the appropriate instruments at the location of the site. On-site measured irradiance data is not available at the project site. Therefore, several meteorological databases with different

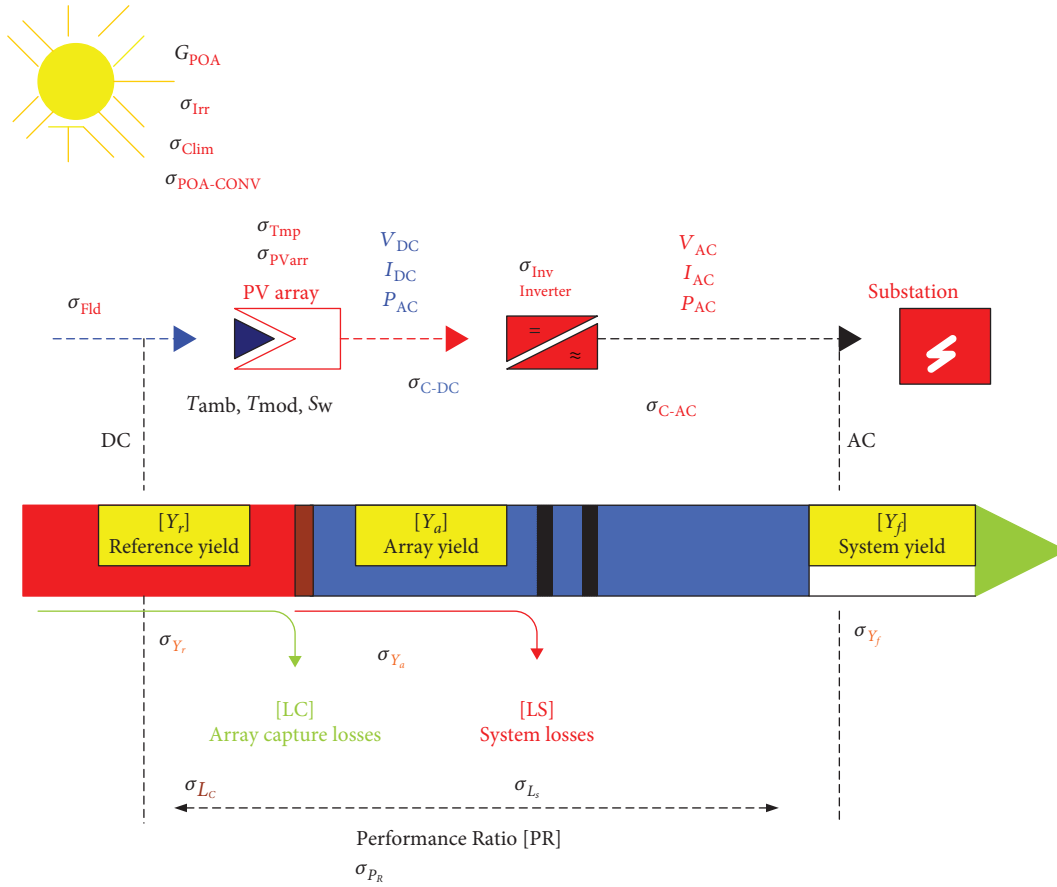


FIGURE 2: Energy yield flow in PV modeling chain parameters are subjected to uncertainties.

quality of data have been used to determine the long-term annual irradiation at the project site [12]. The authors consulted several weather databases as well as data supplied by the client and have obtained irradiation and temperature data from the ones listed in Table 2. The absence of usable on-site irradiance and temperature measurements introduces additional uncertainty in the solar resource assessment.

1.5.1. NASA's Surface Meteorology and Solar Energy Server (NASA-SSE). NASA-SSE can provide the monthly average values from 22 years of collecting data. Irradiation data for global horizontal, diffuse horizontal, and direct normal are provided for the specific coordinates of the site [13]. Table 3 presents the monthly values of global horizontal irradiation (GHI) and ambient temperature obtained from the site.

1.5.2. Meteonorm. Meteonorm is primarily a method for the calculation of solar radiation on arbitrarily orientated surfaces at any specific location [14]. The Meteonorm database is mainly based on the GEBA ground stations and interpolates between the ground stations which we used to estimate the irradiation at the project site [12]. The results of Meteonorm were extrapolated from the Karachi weather station located 105 km from the project site. The coordinates, elevation, and climatic distance are provided in Table 4 below.

Tables 5 and 6 present the average monthly values of the GHI and ambient temperature obtained from Metronome for the project location and the Karachi weather station as well as the period of record of each data, respectively.

1.5.3. SolarGIS. We procured SolarGIS irradiance and temperature data from GeoModel which includes 15 years of meteorological history at the project site. Table 7 presents the average monthly values of the GHI and ambient temperature obtained from SolarGIS for the project location including the period of record [15]. From this data set, the interannual variability of the project site was calculated to be 3.4%.

1.6. Solar Resource Assessment Results. In the absence of an on-site solar monitoring station, the irradiation data sources referred to present several drawbacks. When compared to a high-quality on-site monitoring station, the data sources are lacking accuracy in terms of spatial distance, spatial resolution, or temporal resolution. It should be noted that there are no measured solar radiation data within 25 km of the project site. The GoP and the relevant department are known in this concept and are relying on satellite data to manifest the solar resource assessment studies. We have analyzed each available GHI data source and utilized the data sources to estimate the global horizontal radiation and temperature for the project site. This is because the energy yield of the



FIGURE 3: Physical condition of site/land milestone.

TABLE 1: 3×50 MW project site coordinates.

| Location: Karachi, Pakistan | | |
|-----------------------------|-------------------------------------|------------------|
| Latitude | 25°19'9.1"N | Land coordinates |
| Longitude | 68°4'20.3"E | |
| Elevation | Approximately 112 m above sea level | |

TABLE 2: List of meteorological databases consulted for the project.

| Database | Range | Stations |
|-----------|-----------|--|
| NASA-SSE | Worldwide | Satellites (1 degree longitude \times 1 degree latitude mesh grid) |
| Meteonorm | — | 8,055 weather stations |
| GeoModel | — | Satellite-derived solar radiation |
| SolarGIS | — | and meteorological data |

project site is directly related to the availability of GHI [16]. A summary of the decision-making process is given briefly below.

- (i) The measured data is not available near the project site, but data from surrounding databases have been considered
- (ii) NASA-SSE predicts irradiation data at the project site; however, the data are coarse in spatial resolution with relatively high uncertainty (10%)
- (iii) Meteonorm results are based on extrapolation of data from a weather station located 105 km from the project. The irradiation data have an uncertainty of 11% and with an interannual variability of 4.5%

TABLE 3: Monthly values from NASA-SSE.

| Location | Project site | |
|-----------|---|------------------|
| | Global horizontal irradiation (keh/m ²) | Temperature (°C) |
| Period | 1983-2005 | 1983-2005 |
| January | 118 | 17.6 |
| February | 127 | 19.9 |
| March | 164 | 24.7 |
| April | 189 | 28.3 |
| May | 207 | 30.4 |
| June | 201 | 30.2 |
| July | 179 | 29 |
| August | 168 | 28.3 |
| September | 159 | 28.2 |
| October | 146 | 27.9 |
| November | 188 | 23.9 |
| December | 111 | 19.4 |
| Total | 1887 | 25.7 |

- (iv) SolarGIS data are provided at the project site using satellite data interpolated by the GeoModel algorithm which typically has an uncertainty between 3.5% and 7.0%. The irradiation data for the project site has an estimated uncertainty of 6.0% with a calculated interannual variability of 3.4% [5]

Based on the conclusions above, SolarGIS irradiation has been retained for the analysis based on its lower relative uncertainty, the long period of record, and the representativeness of the project site. The authors consider this source as the best available source of irradiation data for the site and suitable at this stage in the development of the project.

TABLE 4: The coordinates of the Meteonorm stations and climatic distance to the site.

| | Latitude (degree) | Longitude (degree) | Elevation (m) | Climate distance (km) |
|-------------------------|-------------------|--------------------|---------------|-----------------------|
| Karachi weather station | 24.9° N | 67.0° E | 22 | 105 |

TABLE 5: Monthly values of GHI and temperature from Meteonorm from the project site.

| Location | Project site | |
|----------|---|------------------------------------|
| | GHI (kWh/m ²) (interpolated) | Temperature (°C) (interpolated) |
| Period | 1986-2005 | 2000-2009 |
| Jan | 128 | 18.2 |
| Feb | 130 | 21.4 |
| Mar | 164 | 26.0 |
| Apr | 177 | 29.6 |
| May | 189 | 31.9 |
| Jun | 183 | 32.5 |
| Jul | 161 | 31.1 |
| Aug | 162 | 29.9 |
| Sep | 177 | 29.9 |
| Oct | 158 | 28.7 |
| Nov | 129 | 24.2 |
| Dec | 115 | 19.6 |
| Total | 1873 | 26.9 |

TABLE 6: Monthly values of GHI and temperature from the Meteonorm from the nearest weather station.

| Location | Nearest weather station | |
|----------|---|------------------------------------|
| | GHI (kWh/m ²) (interpolated) | Temperature (°C) (interpolated) |
| Period | 1986-2005 | 2000-2009 |
| Jan | 126 | 19.5 |
| Feb | 127 | 22.4 |
| Mar | 164 | 26.4 |
| Apr | 184 | 29.4 |
| May | 192 | 30.8 |
| Jun | 181 | 31.5 |
| Jul | 148 | 30.2 |
| Aug | 148 | 29.1 |
| Sep | 168 | 29.3 |
| Oct | 160 | 29.0 |
| Nov | 125 | 25.2 |
| Dec | 112 | 20.9 |
| Total | 1835 | 27.0 |

Based on its experience, PV projects have progressed through project development using modeled solar resource data with a similar level of uncertainty as the SolarGIS data chosen for this project site.

TABLE 7: Monthly values of GHI and temperature from SolarGIS.

| Period | GHI (kWh/m ²) | Temperature (°C) |
|--------|---------------------------|------------------|
| | 1999-2013 | 1999-2013 |
| Jan | 134 | 18.5 |
| Feb | 153 | 22.7 |
| Mar | 197 | 26.0 |
| Apr | 215 | 32.3 |
| May | 227 | 34.2 |
| Jun | 204 | 33.7 |
| Jul | 180 | 33.7 |
| Aug | 179 | 31.1 |
| Sep | 179 | 31.0 |
| Oct | 172 | 30.0 |
| Nov | 136 | 25.8 |
| Dec | 122 | 20.5 |
| Total | 2098 | 28.3 |

2. Uncertainty Methodology

Solar resource assessment with uncertainty analysis is required to know the mechanism of uncertainty methodology. The methodology of the uncertainty of solar resource is associated with a modeling chain in which the uncertainty term in this paper refers to the RMSE classified as the estimation of a quantity. The RMSE is framed by a systematic part such as MBE and another nonsystematic part “ σ .” The σ is the standard deviation of the error which represents random contributions to the error around the mean value [17]. The term accuracy measures RMSE, MBE, and MAE are normalized over the average value of θ_i which are described as P_{RMSE} , P_{MBE} , and P_{MAE} , respectively; θ_i is the actual quantity, $\bar{\theta}_i$ is the estimated quantity, and P variable is the number of samples which are defined below.

$$\begin{aligned} \text{RMSE} &= \sqrt{\frac{1}{P} \sum_{i=1}^P (\bar{\theta}_i - \theta_i)^2}, \\ \text{MBE} &= \frac{1}{P} \sum_{i=1}^P (\bar{\theta}_i - \theta_i), \\ \text{MAE} &= \frac{1}{P} \sum_{i=1}^P |\bar{\theta}_i - \theta_i|. \end{aligned} \quad (1)$$

Then,

$$\text{RMSE}^2 = \text{MBE}^2 + \sigma^2. \quad (2)$$

TABLE 8: Energy assessment results through simulation.

| | | | | | |
|--------------------------|---|---|-------------------------|--------------------|-----------------------|
| Software | PVSYST V6.47 | | | | |
| Project | 3 × 50 MW solar PV power project | | | | |
| Aggregate power | 50 MW (1 × 50 MW) | | | | |
| Data sources | Meteonorm 7.1 [2001-2010] Sat = 56% | | | | |
| Land coordinates | Longitude 68°4.2', north latitude 25°19.2', altitude 70 m | | | | |
| Legal time | Time zone TU + 5 | | | | |
| Mounting structure | Fixed tile | | | | |
| | PV field orientation | PV modules | PV array | Inverter | User's needs |
| PV system grid-connected | Tilt 20°, azimuth 0° | Model JKM300P-72 Jinko Solar | No. of module 166680 | Model TC 1000KS | Unlimited load (grid) |
| | | Pnom 300 Wp | Pnom total 50004 kWp | Pnom 1000 kW AC | |
| Inverter pack | | No. of units: 50.0, Pnom total: 50000 kW AC | | | |
| PV modules | | 8334 strings of 20 modules in series, 50004 kWp total | | | |
| Area | | 323069 m ² | | | |
| Production | | 80085 MWh/year | | | |
| PR | | 77.62% (performance ratio) | | | |
| No shading field defined | | | | | |

After that,

$$\bar{\theta}_i = \frac{1}{P} \sum_{i=1}^P \theta_i. \quad (3)$$

Here, these values are normalized over the average value

$$P_{\text{RMSE}} = \frac{\text{RMSE}}{\bar{\theta}_i}, \quad (4)$$

$$P_{\text{BME}} = \frac{\text{MBE}}{\bar{\theta}_i}.$$

(N) is presented herein as normalized:

$$P_{\text{MAE(N)}} = \frac{\text{MAE}}{\bar{\text{GI}}}. \quad (5)$$

Here, we define the combination of uncertainty.

The overall role of propagation of uncertainties U_x and U_y for a given function $f(x, y)$ can be computed in equation (6) when we assume the independent variables or neglecting correlations. The equation U_c is an estimation of the standard deviation of the function $f(x, y)$, accepting that U_x and U_y are small compared to the partial derivatives. The combined standard uncertainty U_c is computed using equation (7) based on uncertainty sources which shall be considered independent. In this way, combined expanded uncertainty \vec{U} will be calculated by multiplying the combined standard uncertainty U_c with a coverage factor presented in equation (8). We assume the 96% confidence

interval of Gaussian distribution, and then this coverage factor $\text{Cov}_{\text{Factor}}$ is 1.97. Therefore, the final equation to find the expanded uncertainty \vec{U} is obtained in equation (9) [18].

$$U_c = \sqrt{\left(\frac{\partial f}{\partial x}\right)^2 \cdot U_{x^2} + \left(\frac{\partial f}{\partial y}\right)^2 \cdot U_{y^2}}, \quad (6)$$

$$U_c = \sqrt{\frac{(R_{\text{Norm}_a}/2)^2 + (R_{\text{Uni}_b}/3)^2 + \dots}{P} + \left(\frac{\text{Syst}_{\text{Norm}_c}}{2}\right)^2 + \left(\frac{\text{Syst}_{\text{Uni}_d}}{2}\right)^2 + \dots}. \quad (7)$$

Then, according to equation (7) and $\text{Cov}_{\text{Factor}}$,

$$\vec{U} = \text{Cov}_{\text{Factor}} \cdot U_c. \quad (8)$$

Here, $\text{Cov}_{\text{Factor}} = 1.97$ (coverage factor).

$$\vec{U} = 1.97 \cdot U_c, \quad (9)$$

wherein

U_c = combined uncertainty

\vec{U} = expanded uncertainty

P = number of samples

R_{Norm_a} = normally distributed random components

R_{Uni_b} = uniformly distributed random components

$\text{Syst}_{\text{Norm}_c}$ = normally distributed systematic components

$\text{Syst}_{\text{Uni}_d}$ = uniformly distributed systematic components

3. Results and Discussion

3.1. PV Energy Production. The main simulation results of the energy production produce 80085 MWh/year, and the

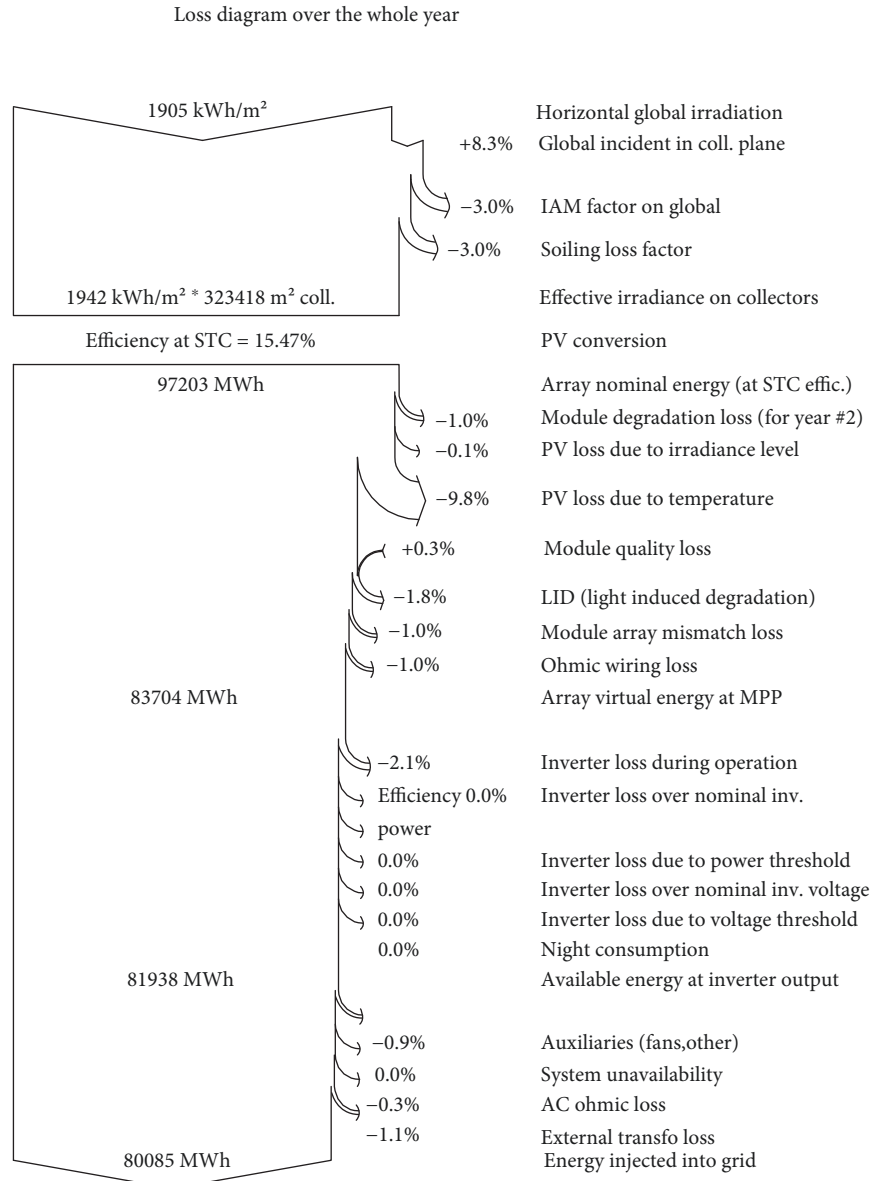


FIGURE 4: Simulation results of losses over the whole year at the PV facility.

performance ratio (PR) of 77.62% is obtained for 1×50 MW from 3×50 MW. These are three (3) 50 MW AC solar projects located adjacent to the same extended piece of land with a combined AC capacity of 150 MW. Therefore, each 50 MW is identical from 3×50 MW, and the (1) 50 MW size is executed for the simulation in this paper. The energy assessment result through simulation is shown in Table 8.

3.1.1. Loss Diagram. According to the simulation result of the loss diagram in Figure 3, PV facility defined loss factors such as module quality of +0.3%, module degradation loss of -1.0%, soiling of -0.3%, mismatch of -0.1, cabling (ohmic wiring loss) of -0.1%, inverter efficiency of -2.1%, transformer of -1.1%, system availability of 0.0%, and grid availability and parasitic [18, 19]. Based on the PV correction, the array nominal energy is defined as 9723 MW/h at an STC efficiency of 15.47% as well as array virtual energy

at MPPT which is calculated at 83704 MW/h. Before the final energy is injected into the grid, available energy at the inverter output side is assumed significant in whole losses in the PV system; therefore, the energy in the inverter output is calculated as 81938 MW/h. The final energy is injected into grid 80085 MW/h which predicts the estimated Figure 4 after all losses behavior done.

The results of Figures 5–8 show the energy flow in the PV system defining the losses at each step and setting the benchmark of energy. Figures 9 and 10 show the energy injected into the grid monthly based on the daily input/output energy diagram.

3.2. Uncertainty Analysis. The uncertainty of the final result is a consequence of the uncertainty of solar radiation in this case (global horizontal irradiation), the inaccuracies of the simulation procedure itself (a choice of model), and

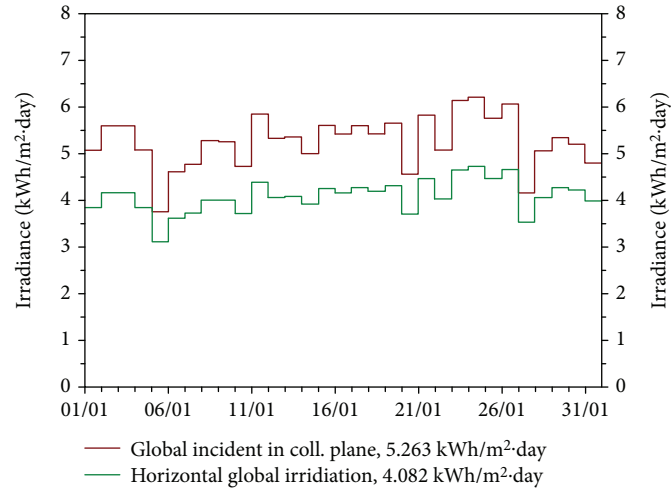


FIGURE 5: First month values of horizontal global irradiation and global incident in coll. plane.

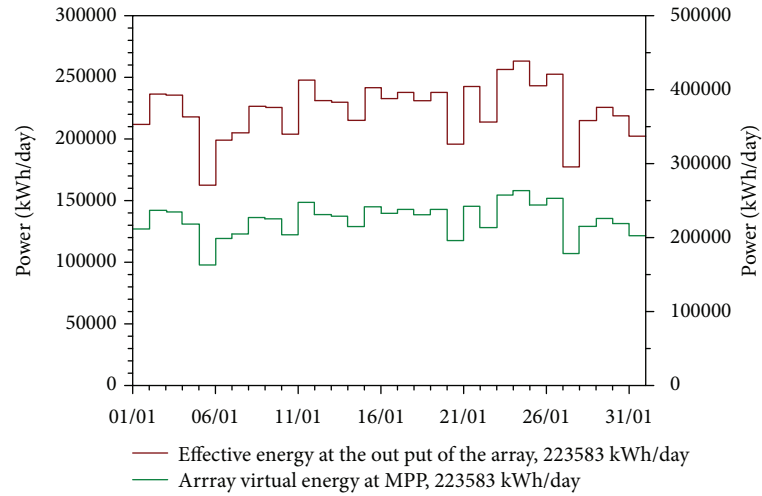


FIGURE 6: First month effective energy at the output of the array and array virtual energy at MPPT.

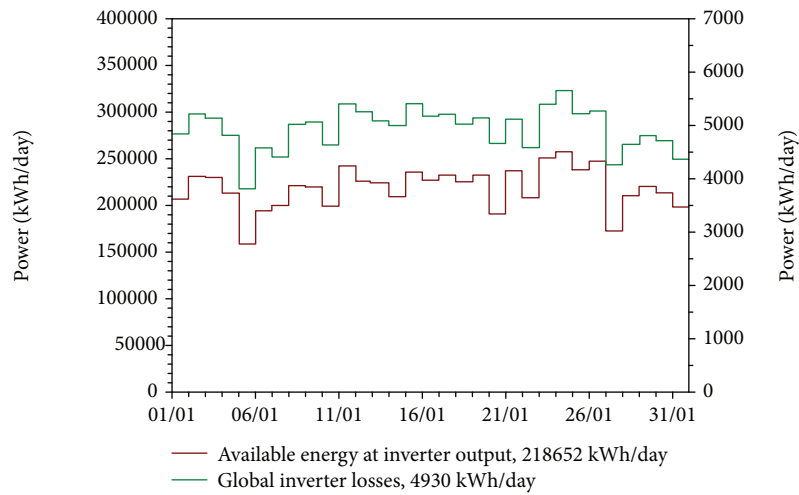


FIGURE 7: First month of global inverter loss and available energy at inverter output.

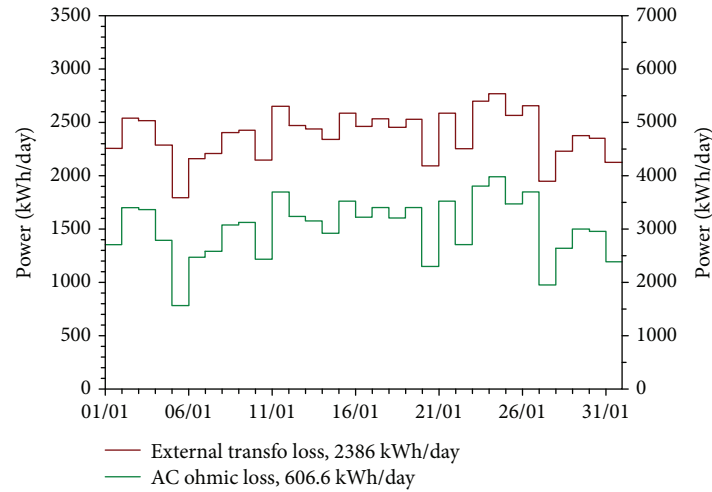


FIGURE 8: First month AC ohmic loss and external transformer loss.

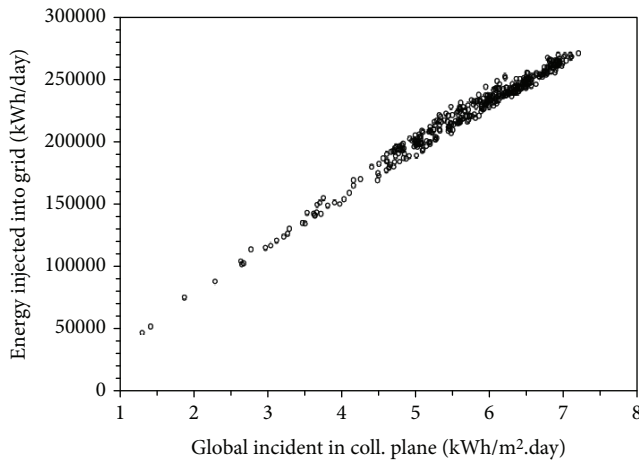


FIGURE 9: Daily input/output energy diagram.

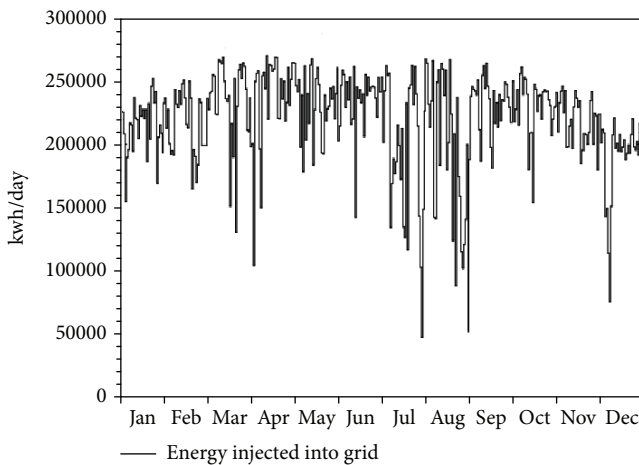


FIGURE 10: Energy injected into the grid monthly.

uncertainties associated with external influences (shading, soiling, deviation of components from specification, inverter losses, cabling losses, etc.).

TABLE 9: The above sources assessed for the project and are presented in the table.

| Source of uncertainty in the simulation | Estimated uncertainty standard deviation |
|---|--|
| Irradiation on the tilted plane | 3.0% |
| Shading/soiling/snow | 2.5% |
| Reflection and spectral losses | 1.5% |
| Deviation from STC | 4.0% |
| Module power tolerance | 2.0% |
| Module mismatch | 1.0% |
| Cabling losses | 0.8% |
| MPPT tracking | 0.5% |
| Inverter losses | 1.5% |
| Total | 6.4% |

TABLE 10: The uncertainty figures considered for the project.

| PV plant | | | |
|----------------------------|----------|--------------------------------|----------|
| Simulation uncertainty (%) | | Solar resource uncertainty (%) | |
| 6.4% | | 6.1% | |
| Future variability (%) | | Total uncertainty (%) | |
| 1 year | 10 years | 1 year | 10 years |
| 3.4% | 1.1% | 9.5% | 8.9% |

3.2.1. Uncertainty Analysis of the Irradiation Data. Variability of the global horizontal irradiation is not negligible; at this site, the interannual variability of 3.4% of the project area has been calculated based on 15 years of monthly GI data from SolarGIS. In addition to the yearly variability of GHI, we have estimated an uncertainty of 6.0%–6.1% to account for any error in the modeled GHI data. This uncertainty considers the modeling accuracy of GHI data for the project site considering the vendor validation results of the model within this region.

TABLE 11: Confidence limits for the PV layout of PV plant 1- and 10-year periods, without power degradation.

| Probability of exceedance (%) | 1 year | | 10 years | |
|-------------------------------|-------------------------------|---------------------------|-------------------------------|---------------------------|
| | Net energy output (MWh/annum) | Capacity factor (%/annum) | Net energy output (MWh/annum) | Capacity factor (%/annum) |
| 99 | 86,683 | 15.3% | 88,146 | 15.5% |
| 90 | 97,700 | 17.2% | 98,506 | 17.4% |
| 75 | 104,101 | 18.3% | 104,525 | 18.4% |
| 60 | 108,542 | 19.1% | 108,701 | 19.1% |
| 50 | 111,213 | 19.6% | 111,213 | 19.6% |
| 25 | 118,325 | 20.8% | 117,900 | 20.8% |
| Total | 104,761 | 18.4% | 104,832 | 18.5% |

(1) *Uncertainty of the Simulation.* The main sources of uncertainties, excluding the variability of the global horizontal irradiation, are as shown in Table 9.

(2) *Total Uncertainty.* The future variability of GHI should be added to the above uncertainties, in order to obtain the total uncertainty in the solar energy assessment. The one-year or ten-year periods are typically under consideration. It is assumed that all errors are independent and that the Gaussian distribution is applicable. Table 10 resumes the uncertainty figures considered for the project.

The total uncertainty of the energy production estimate could be reduced by considering an on-site solar monitoring station with irradiance data measured for a minimum period of one year. The confidence limits for probabilities of exceeding 99%, 90%, 75%, 60%, and 50% for the one year and ten years are provided in Table 11 for each layout in downside scenarios. Additionally, we have an “upside” probability exceeding 25% in Table 11.

The capacity factor of a PV plant is defined as the ratio of the actual energy produced over a period of time, to the hypothetical maximum possible, which refers to running full time at a rated power [19–21].

3.3. Power Degradation and Production. The degradation factors based on the PV module manufacturer’s warranty are typically pessimistic, and a more realistic approach on the temperature of the photovoltaic module has an adverse effect on the performance of photovoltaic modules [22]. If degradation is less, then good performance depends on the environmental conditions and seasons of the year. Previous research depicts that modules of different technologies have shown par. It has to be based on both the track record and existing information regarding each technology of the PV module’s manufacture. For that purpose, the polycrystalline silicon technology track record is taken into consideration. Ideally, module degradation would be further investigated during the technical due diligence process for the project, and the analysis of the specific datasheet would be reviewed by the module manufacturer. The authors have considered the PV module technology track record. Based on this review, the authors applied a linear factor of 0.75% to account for annual degradation due to long-term mechanisms. The degradation factor at the end of a single year is applied at the beginning of

TABLE 12: Performance ratio and net energy output (MWh/year) for one-year periods.

| Year | PR (%) | P25 | P50 | P75 | P90 | P99 |
|-------|--------------|----------------|-----------------|----------------|----------------|----------------|
| 1 | 77.6 | 122750 | 115383 | 108006 | 101365 | 90064 |
| 2 | 77.2 | 121870 | 114549 | 107225 | 100632 | 89414 |
| 3 | 76.80 | 121099 | 113715 | 106444 | 99899 | 88764 |
| 4 | 76.20 | 120102 | 112881 | 105663 | 99166 | 88114 |
| 5 | 75.90 | 119214 | 112047 | 104882 | 98433 | 87464 |
| 6 | 75.50 | 118326 | 111213 | 104101 | 97700 | 86683 |
| 7 | 75.10 | 117438 | 110379 | 103320 | 96967 | 86033 |
| 8 | 74.50 | 16550 | 109545 | 102539 | 96234 | 85383 |
| 9 | 73.90 | 15663 | 108711 | 10 1759 | 95502 | 84733 |
| 10 | 73.40 | 14775 | 107877 | 10 0978 | 94769 | 84083 |
| 11 | 72.80 | 13888 | 107042 | 100197 | 94036 | 83433 |
| 12 | 72.20 | 13000 | 106208 | 99416 | 93,303 | 82782 |
| 13 | 71.70 | 12113 | 105374 | 98636 | 92571 | 82132 |
| 14 | 71.10 | 11225 | 104540 | 97855 | 91838 | 81482 |
| 15 | 70.50 | 10338 | 103706 | 97074 | 91105 | 80832 |
| 16 | 70.00 | 9451 | 102872 | 96293 | 90372 | 80182 |
| 17 | 69.40 | 8563 | 102038 | 95513 | 89640 | 79532 |
| 18 | 68.80 | 7676 | 101204 | 94732 | 88907 | 78882 |
| 19 | 68.30 | 6788 | 100370 | 93951 | 88174 | 78232 |
| 20 | 67.70 | 5901 | 99536 | 93170 | 87441 | 77581 |
| 21 | 67.10 | 5013 | 98701 | 92390 | 86709 | 76931 |
| 22 | 66.60 | 4126 | 97867 | 91609 | 85976 | 76281 |
| 23 | 66.00 | 3239 | 97033 | 90828 | 85243 | 75631 |
| 24 | 65.40 | 2351 | 96199 | 90047 | 84510 | 74981 |
| 25 | 64.90 | 1464 | 95365 | 89267 | 83778 | 74331 |
| Total | 71.54 | 40116.9 | 105374.2 | 94341.5 | 92570.8 | 82158.4 |

the same year, based on a pragmatic approach [5]. As a result, the PR for each single year is demonstrated in Table 12. The resulting production figures for a one-year period, with corresponding performance ratios, are also presented in Table 12. In order to reduce the minimum degradation factor in PV panels, a regular cleaning mechanism is required to enhance the good production [23]. The PV module degradation losses can reach 5% with a lifespan of 20~25-year warranty period [19, 24].

4. Conclusion

The authors evaluated the energy yield assessment with a study of different solar resources, which is based on uncertainty analysis for acquiring the final selection of the equipment and technology choice. Based on the total estimated production by simulation, the performance ratio of 77.62% and CF of 18.2% are calculated. However, based on the total uncertainty analysis, the net energy output/year and capacity factor/year are calculated at P99, P90, P75, P60, P50, and P25 and are presented in Table 11. We applied a linear factor of 0.75% to account for the annual degradation (1~25 years) at the different probability of exceedance due to the long-term mechanisms applied. As a result, total PR% and total production at P25, P50, P75, P90, and P99 are calculated and presented in Table 12. In these results, we found that the PV plant is still achievable and the system can inject the target production into the grid, which will be given less PR shortfall against liquidated damages and fulfill the requirements of the power warranty.

Nomenclature

| | |
|-------------------|---|
| PV: | Photovoltaic |
| PR: | Performance ratio |
| MPPT: | Maximum power point tracker |
| CF: | Capacity factor |
| GoP: | Government of Pakistan |
| LoI: | Letter of intent |
| IPPs: | Independent power producers |
| CO ₂ : | Carbon dioxide |
| IA: | Implementation of agreement |
| RE: | Renewable energy |
| MW: | Megawatt |
| AC: | Alternative current |
| DC: | Direct current |
| PVsyst: | Photovoltaic System Software |
| KV: | Kilovolts |
| NASA-SEE: | NASA's Surface Meteorology and Solar Energy |
| GHI: | Global horizontal irradiation |
| GI: | Global irradiation |
| RMSE: | Root mean square error |
| MBE: | Mean bias error |
| MAE: | Mean absolute error |
| GBEA: | Global energy balance archive |
| STC: | Standard temperature condition. |

Data Availability

The data used to support the findings of this study are available from the corresponding author upon request.

Conflicts of Interest

The authors declare that they have no conflict of interest with regard to publishing this article.

Acknowledgments

This work was supported by the State Key Research Project (2017YFB0902600) and by the National Natural Science Foundation of China under Grant No. 51577049. The authors thank TBEA Xinjiang Sunoasis Co. Ltd., for the support in facilitating our conducting the experiments on site and for data acquisition.

References

- [1] R. Jamil, M. Li, X. Ji, and X. Luo, "An overview of photovoltaic power generation and solar PV technology in rural area of Pakistan," in *Proceedings of 26th Ecos*, Guilin, China, 2013.
- [2] H. A. Muhammad, M. Mahmood, M. Bashir Anser, M. Ali, and A. Siddiqui Maryam, "Outdoor testing of photovoltaic modules during summer in Taxila, Pakistan," *Thermal Science*, vol. 20, no. 1, pp. 165–173, 2016.
- [3] M. A. Bashir, H. M. Ali, S. Khalil, M. Ali, and A. M. Siddiqui, "Comparison of performance measurements of photovoltaic modules during winter months in Taxila, Pakistan," *International Journal of Photoenergy*, vol. 2014, Article ID 898414, 8 pages, 2014.
- [4] M. A. Eltawil and Z. Zhao, "Grid-connected photovoltaic power systems: technical and potential problems—a review," *Renewable and Sustainable Energy Reviews*, vol. 14, no. 1, pp. 112–129, 2010.
- [5] I. Jamil, J. Zhao, L. Zhang, R. Jamil, and S. F. Rafique, "Evaluation of energy production and energy yield assessment based on feasibility, design, and execution of 3 × 50 MW grid-connected solar PV pilot project in Nooriabad," *International Journal of Photoenergy*, vol. 2017, Article ID 6429581, 18 pages, 2017.
- [6] B. Goss, R. Gottschalg, and T. R. Betts, "Uncertainty analysis of photovoltaic yield prediction," *8th photovoltaic science application and technology (PVSTAT-8) Conference Exhibition*, 2012, pp. 157–160, Newcastle England, April 2012.
- [7] M. Richter, K. De Brabandere, J. Kalisch, T. Schmidt, and E. Lorenz, *Best Practice Guide On Uncertainty in PV Modelling*, University of Oldenburg, 2015.
- [8] A. Ioannou, A. Angus, and F. Brennan, "Risk-based methods for sustainable energy system planning: a review," *Renewable and Sustainable Energy Reviews*, vol. 74, pp. 602–615, 2017.
- [9] T. Mahachi, "Energy yield analysis and evaluation of solar irradiance models for a utility scale solar PV plant in South Africa," Thesis of Stellenbosch University, 2016.
- [10] M. Zhao, Z. Liu, and Y. Mingjun, "Testing and analyzing of solar energy resource assessment in inner Mongolia," in *2009 4th IEEE Conference on Industrial Electronics and Applications*, Xi'an, China, May 2009.
- [11] M. Zha, Z. Liu, and M. Yu, "Data acquisition and analyzing of solar energy resource," in *The 2010 IEEE International Conference on Information and Automation*, Harbin, China, June 2010.
- [12] C. Budig, J. Orozaliyev, and K. Vajen, "Comparison of different sources of meteorological data for Central Asia and Russia," in *12th International Conference on Solar Energy for Buildings and Industry*, Graz, Austria, September 2018.
- [13] NASA SSE, *Surface Meteorology and Solar Energy (SSE) Release 6.0- Methodology Version 2.4*, NASA Prediction of Worldwide Energy Resource (POWER), 2009.

- [14] W. Moustafa and I. Hegazy, "Towards a sufficient building performance in Egypt: investigating the effect of climatic data types," *International Journal of Scientific & Engineering Research*, vol. 4, no. 6, 2013.
- [15] I. B. Schnierer and A. Skoczek, *Energy Yield Assessment of the Photovoltaic Power Plant*, Solargis S.R.O, 2013, sample report.
- [16] I. Loghmari and Y. Timoumi, "Improvement global solar radiation estimation," *IET Renewable Power Generation*, vol. 11, no. 7, pp. 996–1004, 2017.
- [17] D. Thevenard and S. Pelland, "Estimating the uncertainty in long-term photovoltaic yield predictions," *Solar Energy*, vol. 91, pp. 432–445, 2013.
- [18] E. Kymakis, S. Kalykakis, and T. M. Papazoglou, "Performance analysis of a grid connected photovoltaic park on the island of Crete," *Energy Conversion and Management*, vol. 50, no. 3, pp. 433–438, 2009.
- [19] K. Attari, A. Elyaakoubi, and A. Asselman, "Performance analysis and investigation of a grid-connected photovoltaic installation in Morocco," *Energy Reports*, vol. 2, pp. 261–266, 2016.
- [20] J. Fouladgar, "A stochastic model for power and storage selection of wind systems," in *2011 10th International Conference on Environment and Electrical Engineering*, Rome, Italy, May 2011.
- [21] Y. Yihdego, H. S. Salem, and M. Y. Pudza, "Renewable energy: wind farm perspectives—the case of Africa," *Journal of Sustainable Energy Engineering*, vol. 5, no. 4, pp. 281–306, 2017.
- [22] B. M. Anser, A. H. Muhammad, A. K. Pervez et al., "Performance investigation of photovoltaic modules by back surface water cooling," *Thermal Science*, vol. 21, no. 2, p. 290, 2017.
- [23] H. A. Muhammad, M. Z. Abdullah, M. B. Anser, M. N. Ali, M. Ali, and A. S. Maryam, "Effect of dust deposition on the performance of photovoltaic modules in Taxila, Pakistan," *Thermal Science*, vol. 21, no. 2, pp. 915–923, 2017.
- [24] E. D. Dunlop, "Lifetime performance of crystalline silicon PV modules," in *Proceedings of 3rd World Conference on Photovoltaic Energy Conversion*, 2003, pp. 2927–2930, Osaka, Japan, May 2003.

